

Min Gu

# Advanced Optical Imaging Theory

With 93 Figures



Springer

## *Chapter 3*

# **POINT SPREAD FUNCTION ANALYSIS**

In the classic optical imaging theory of a lens [3.1, 3.2], discussions on imaging performance of a lens are usually limited to thin objects because conventional optical microscopy provides a two-dimensional (2-D) image of a thin sample. However, confocal microscopy exhibits an optical sectioning property [3.3] which allows one to perform three-dimensional (3-D) imaging of a sample with depth structures. The 3-D imaging property, or the 3-D light distribution near the focus, of an objective lens is also important in laser trapping technology [3.4]. All of these new developments require a better understanding of the performance of a lens along the axial direction. This chapter is to study diffraction properties of a single lens in the focal region under the paraxial approximation introduced in Section 2.4. A discussion on the same topic without this approximation can be found in Chapter 6. There are two ways for analysing the imaging performance of a lens, the point spread function method and the transfer function method. The former, relatively simple in terms of the mathematical skills involved, is based on the image of a single point object and is the topic of the current chapter, while a detailed discussion based on the transfer function method will be given in the next chapter.

This chapter is arranged as follows. An expression for the transmittance of a single lens is derived in Section 3.1. With this expression, the Fresnel diffraction formula in Eq. (2.4.5) is employed in Section 3.2 to study 3-D diffraction patterns by various lenses. In Section 3.3, the point spread function (PSF) for a lens for coherent image formation is given for a thin object. This method is generalized to imaging an object of finite thickness in Section 3.4, after the 3-D space invariant PSF for a lens is derived. Finally, incoherent image formation of a lens is presented in Section 3.5.

### **3.1 Transmittance of a Single Lens**

When a light wave of wavelength  $\lambda$  passes through an optical lens formed by two spherical surface as shown in Fig. 3.1.1, two physical changes occur to the light field impinging on the lens. The first change is the phase change of the field due to the change in optical path, and the second is the amplitude change of the field due to the Fresnel re-

reflection and transmission [2.1] on the surfaces of the lens. To study these two effects, we can express the transmittance of a lens as a complex function  $t(x, y)$ , i.e.

$$t(x, y) = \frac{U_2(x, y)}{U_1(x, y)}, \quad (3.1.1)$$

where  $U_1(x_1, y_1)$  and  $U_2(x_2, y_2)$  are the light fields in the planes immediately before and behind the lens, respectively, as shown in Fig. 3.1.1. In particular, we can express  $t(x, y)$  as

$$t(x, y) = P(x, y) \exp[-i\phi(x, y)]. \quad (3.1.2)$$

Here  $P(x, y)$  and  $\phi(x, y)$  are the two functions responsible for the amplitude and phase changes in the incident light, respectively. The function  $P(x, y)$  is sometimes called the pupil function of the lens and confined to the aperture of a lens.

If a lens is optically thin and has the uniform refractive index  $\tilde{n}$ , the displacement of the beam caused by the refraction of the lens surfaces can be neglected, i.e. the coordinates on the front and back surfaces of the lens are the same:

$$x_1 = x_2 = x,$$

$$y_1 = y_2 = y.$$

(3.1.3)

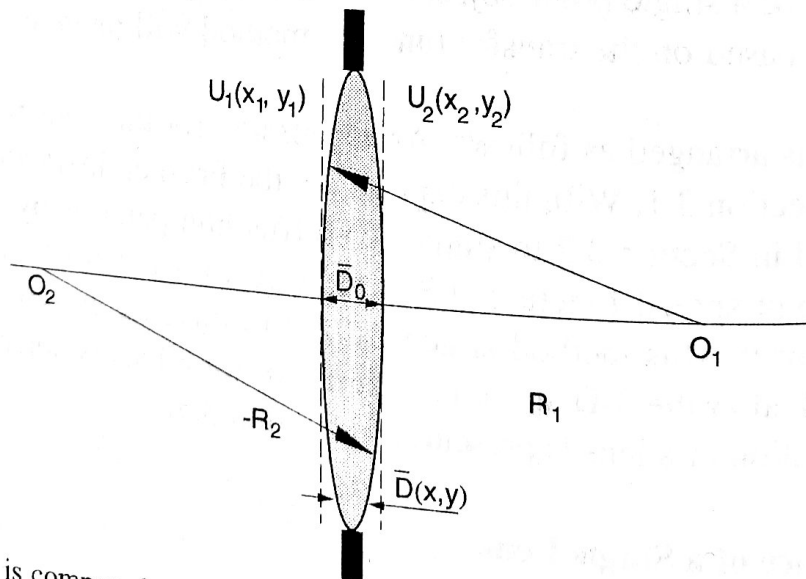


Fig. 3.1.1 A lens is composed of two spherical surfaces with radii of curvature,  $R_1$  and  $-R_2$ , subtended at  $O_1$  and  $O_2$ , respectively. If  $\bar{D}_0$ , the thickness of the lens on the axis, is so small that the displacement of the beam passing through the lens is negligible, such a lens can be considered to be a thin lens.

If the front and back surfaces forming the lens are spherical surfaces with radii of curvature,  $R_1$  and  $-R_2$ , where the negative sign represents that the two surfaces face the opposite directions, and the geometrical thickness of the lens on the optical axis is  $\bar{D}_0$ , the geometrical thickness at any point on the lens,  $\bar{D}(x, y)$ , can be derived according to the geometrical conditions given in Fig. 3.1.1. Under the paraxial approximation (see Section 2.4),  $\bar{D}(x, y)$  can be expressed as

$$\bar{D}(x, y) = \bar{D}_0 - \frac{x^2 + y^2}{2} \left( \frac{1}{R_1} - \frac{1}{R_2} \right). \quad (3.1.4)$$

Multiplying Eq. (3.1.4) by the wave number  $k$  leads to the phase delay caused by the refraction of the lens. Finally, the phase delay from the front surface of the lens to the back surface of the lens becomes

$$\phi(x, y) = k\tilde{n}\bar{D}(x, y) / n + k[\bar{D}_0 - \bar{D}(x, y)], \quad (3.1.5)$$

where  $k = 2\pi/\lambda$  is the wave number of the incident light in the immersion medium (refractive index  $n$ ) of the lens.

Substituting Eqs. (3.1.5) into Eq. (3.1.1), we can obtain

$$U_2(x, y) = U_1(x, y)P(x, y)\exp(-ik\tilde{n}\bar{D}_0 / n) \exp\left[ ik\left(\frac{\tilde{n}}{n} - 1\right) \frac{x^2 + y^2}{2} \left( \frac{1}{R_1} - \frac{1}{R_2} \right) \right], \quad (3.1.6)$$

from which we can introduce

$$\frac{1}{f} = \left( \frac{\tilde{n}}{n} - 1 \right) \left( \frac{1}{R_1} - \frac{1}{R_2} \right). \quad (3.1.7)$$

Here  $f$  is called the focal length of the lens in geometrical optics. Thus the transmittance of the lens is given by

$$t(x, y) = P(x, y)\exp(-ik\tilde{n}\bar{D}_0 / n)\exp\left[ \frac{ik(x^2 + y^2)}{2f} \right]. \quad (3.1.8)$$

The first factor  $\exp(-ik\tilde{n}\bar{D}_0/n)$  represents a constant phase term contributed by a beam along the axis, so that it can be neglected. Finally, the complex transmittance of a thin lens is

$$t(x, y) = P(x, y) \exp \left[ \frac{ik(x^2 + y^2)}{2f} \right]. \quad (3.1.9)$$

It is seen that the phase change caused by a lens shows a quadratic dependence on  $x$  and  $y$ . For a circularly symmetric lens, the quadratic phase change represents that the lens causes either a convergent wave if  $f$  is positive or a divergent wave if  $f$  is negative, which are called the positive and negative lenses, respectively.

For a positive lens, a plane wave, after passing through the lens, converges to a point at a distance  $f$  behind the lens. This point is called the focus of the lens in geometrical optics. However, according to diffraction of light, the distribution of the light field near the focal region is the superposition of the wavelets from the wavefront behind the lens and therefore the light field distributes within a region near the focus. Details of the distribution of the field in the focal region of a lens will be discussed by using the diffraction formula in the next section.

### 3.2 Diffraction by a Lens

In this section, we will consider the detail of the light field near the focal region of a lens. We first consider the light field in the focal plane, i.e. at  $z = f$  (see Fig. 3.2.1). Suppose that a plane wave of amplitude  $U_0$  is incident upon a lens. Thus the field in the plane immediately before the lens is  $U_1(x_1, y_1) = U_0$ . The lens is a diffraction screen of a complex transmittance given by Eq. (3.1.9). Therefore, the field in the plane immediately behind the lens is

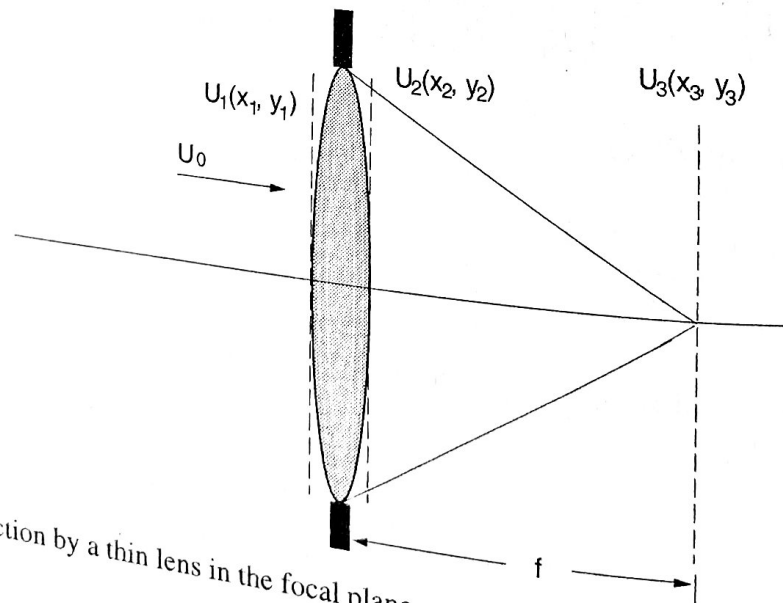


Fig. 3.2.1 Diffraction by a thin lens in the focal plane.

### 3.2 Diffraction by a Lens

$$U_2(x_2, y_2) = U_0 P(x_2, y_2) \exp \left[ \frac{ik}{2f} (x_2^2 + y_2^2) \right]. \quad (3.2.1)$$

So the field in the focal plane can be derived from the Fresnel diffraction formula given in Eq. (2.4.5). Substituting Eq. (3.2.1) into Eq. (2.4.5), we can express the light field in a plane of observation placed at the focus, i.e. at  $z = f$ , as

$$U_3(x_3, y_3) = \frac{iU_0}{\lambda f} \exp(-ikf) \int \int_{-\infty}^{\infty} P(x_2, y_2) \exp \left[ \frac{ik}{2f} (x_2^2 + y_2^2) \right] \exp \left[ -\frac{ik}{2f} (x_3^2 + y_3^2) \right] \exp \left[ -\frac{ik}{f} (x_3 x_2 + y_3 y_2) \right] dx_2 dy_2. \quad (3.2.2)$$

Here the nonlinear phase term in Eq. (2.4.5) has been expanded into three terms in the second line of Eq. (3.2.2). Clearly, the quadratic phase caused by the lens is cancelled out by the quadratic phase resulting from the Fresnel diffraction process, which leads to

$$U_3(x_3, y_3) = \frac{iU_0}{\lambda f} \exp(-ikf) \exp \left[ -\frac{ik}{2f} (x_3^2 + y_3^2) \right] \int \int_{-\infty}^{\infty} P(x_2, y_2) \exp \left[ \frac{ik}{f} (x_3 x_2 + y_3 y_2) \right] dx_2 dy_2. \quad (3.2.3)$$

To explain the physical meaning of Eq. (3.2.3), we let  $m = x_3/(f\lambda)$  and  $n = y_3/(f\lambda)$ . Thus the integration in Eq. (3.2.3) is the two-dimensional (2-D) Fourier transform of the pupil function  $P(x, y)$  at spatial frequencies of  $m$  and  $n$  (see Appendix A). Comparing Eq. (3.2.3) with Eq. (2.4.8), we find that Eq. (3.2.3) gives a Fraunhofer diffraction pattern of  $P(x, y)$  in the focal plane. In other words, to observe the Fraunhofer diffraction by a circular aperture of radius  $a$ , one can use a lens of radius  $a$  and the resulting diffraction pattern in the focal plane has the same distribution as the Fraunhofer diffraction by the circular aperture. It should be pointed out that although  $U_3(x_3, y_3)$  in Eq. (3.2.3) takes a form of the Fraunhofer diffraction of the pupil function, the diffraction process caused by a lens is the Fresnel diffraction rather than the Fraunhofer diffraction.

Now let us turn into the study on the diffraction pattern by a thin lens if the observation plane is placed at a defocus position. Assume the defocus distance to be  $\Delta z$  (see Fig. 3.2.2). The distance between the observation plane and the lens is thus  $z = f + \Delta z$ . For a uniform plane wave  $U_0$  incident upon the lens, the field immediately behind the

lens  $U_2(x_2, y_2)$  is the same as Eq. (3.2.1). Therefore, in terms of the Fresnel diffraction formula (2.4.5), the field  $U_3(x_3, y_3)$  on the observation plane at  $z = f + \Delta z$  is given by

$$U_3(x_3, y_3) = \frac{iU_0}{\lambda z} \exp(-ikz) \iint_{-\infty}^{\infty} P(x_2, y_2) \exp\left[\frac{ik}{2f}(x_2^2 + y_2^2)\right] \exp\left\{-\frac{ik}{2z}[(x_3 - x_2)^2 + (y_3 - y_2)^2]\right\} dx_2 dy_2. \quad (3.2.4)$$

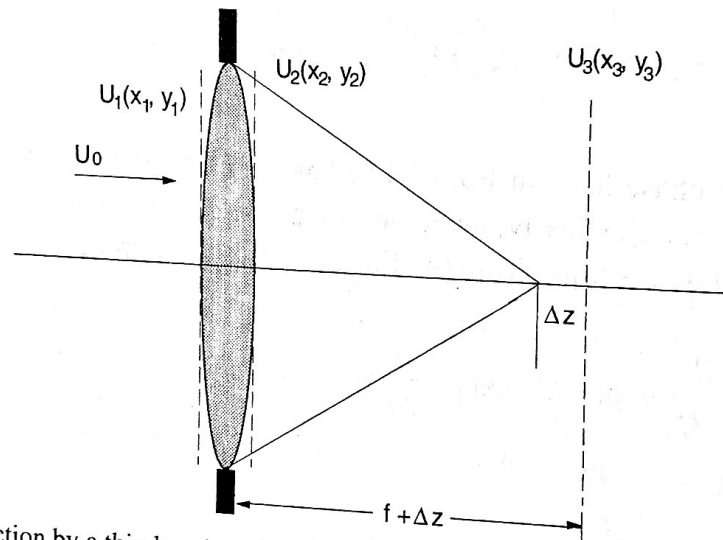


Fig. 3.2.2 Diffraction by a thin lens in a defocus plane.

### 3.2.1 Circular Lens

As mentioned before, a practical lens is usually circularly symmetric. In this case, its pupil function is only a function of the radial coordinate, i.e.  $P(x, y) = P(r)$ , where  $r = (x^2 + y^2)^{1/2}$ . Using a polar coordinate system in Eq. (3.2.3) and the method described in Appendix B, we have

$$U_3(r_3) = \frac{i}{\lambda f} \exp(-ikf) \exp\left(-\frac{i\pi r_3^2}{\lambda f}\right) \int_0^{\infty} P(r_2) J_0\left(\frac{2\pi r r_3}{\lambda f}\right) 2\pi r_2 dr_2, \quad (3.2.5)$$

where we have assumed  $U_0 = 1$ . Here  $J_0$  is a Bessel function of the first kind of order zero,  $r_2 = (x_2^2 + y_2^2)^{1/2}$  and  $r_3 = (x_3^2 + y_3^2)^{1/2}$ . If  $P(r)$  is a uniform circular aperture with radius  $a$ , one can express its pupil function as

$$P(r) = \begin{cases} 1, & r \leq a, \\ 0, & \text{otherwise.} \end{cases} \quad (3.2.6)$$

By using the Hankel transform in Appendix B, we can reduce Eq. (3.2.5) to

$$U_3(r_3) = \frac{i\pi a^2}{\lambda f} \exp(-ikf) \exp\left(-\frac{i\pi r_3^2}{\lambda f}\right) \left[ \frac{2J_1\left(\frac{2\pi r_3 a}{\lambda f}\right)}{\left(\frac{2\pi r_3 a}{\lambda f}\right)} \right], \quad (3.2.7)$$

where  $J_1$  is a Bessel function of the first kind of order unity.

In order to simplify Eq. (3.2.7), we introduce three important parameters.

a) Numerical aperture of the lens, NA:

$$NA = n \sin \alpha \approx n \frac{a}{f}. \quad (3.2.8)$$

The significance of the NA of an objective lens can be found from Fig. 3.2.3; a higher numerical-aperture objective corresponds to a larger maximum angle of convergence,  $\alpha$ . For a given maximum angle of convergence, increasing the refractive index of the immersion medium of a lens yields a high numerical aperture of an objective.

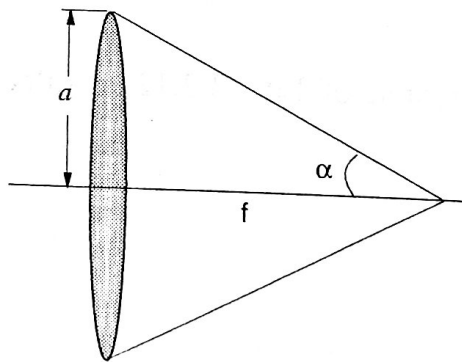


Fig. 3.2.3 Description of the numerical aperture of a lens.

b) Radial (transverse) optical coordinate  $v$ . The definition of the radial optical coordinate is given by

$$v = \frac{2\pi a}{\lambda} \frac{a}{f} r_3 \approx \frac{2\pi}{\lambda} r_3 \sin \alpha. \quad (3.2.9)$$



Therefore for a given value of  $v$ , the larger the numerical aperture of a lens the smaller the value of the real radial coordinate in the focal region.

c) Fresnel number  $N$ :

$$N = \frac{\pi a^2}{\lambda z} \quad (3.2.10)$$

In terms of Eqs. (3.2.8) - (3.2.10), one can rewrite Eqs. (3.2.5) and (3.2.7) as

$$U_3(v) = 2iN \exp(-ikf) \exp\left(-\frac{iv^2}{4N}\right) \int_0^1 P(\rho) J_0(v\rho) \rho d\rho \quad (3.2.11)$$

and

$$U_3(v) = iN \exp(-ikf) \exp\left(-\frac{iv^2}{4N}\right) \left[ \frac{2J_1(v)}{v} \right], \quad (3.2.12)$$

respectively, where  $\rho = r_z/a$  is the normalized radial coordinate over the lens aperture.  $P(\rho)$  is the pupil function with the normalized radius of unity and is given by

$$P(\rho) = \begin{cases} 1 & , \quad \rho \leq 1, \\ 0 & , \quad \text{otherwise,} \end{cases} \quad (3.2.13)$$

for a uniform circular pupil.

Taking the modulus squared of Eq. (3.2.12) results in the intensity in the focal plane:

$$I(v) = (\pi N)^2 \left[ \frac{2J_1(v)}{v} \right]^2. \quad (3.2.14)$$

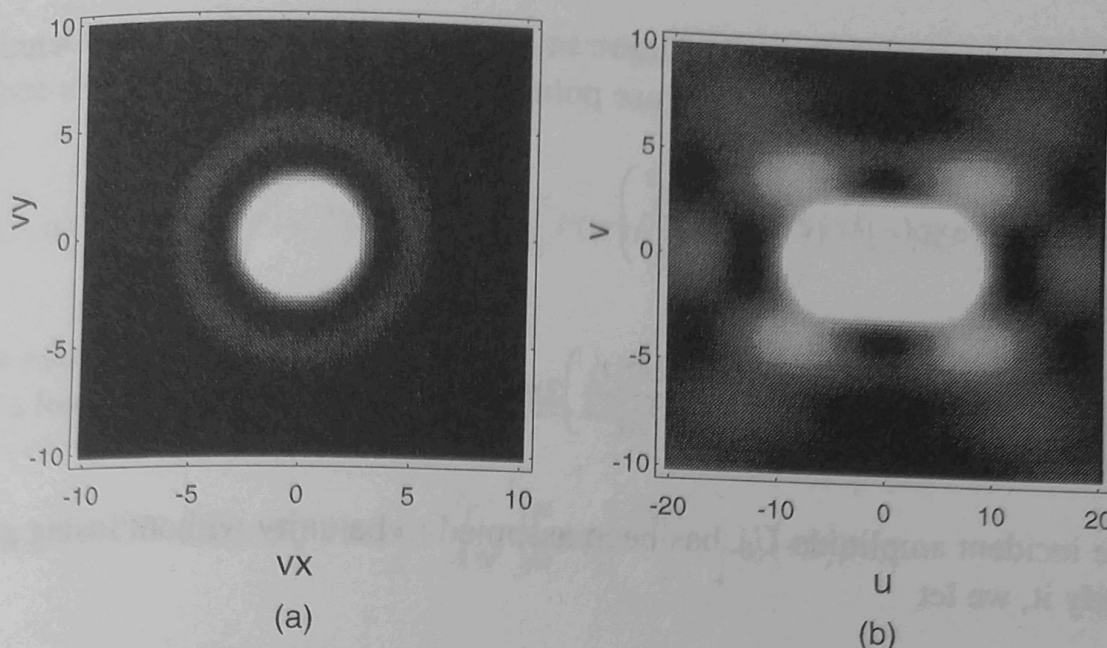


Fig. 3.2.4 Intensity distribution of a single circular lens in the focal plane (a) and in the axial plane including the optical axis near the focus (b). The plot range is within 0 and 0.1 of the intensity normalized by the peak intensity.  $v_x$  and  $v_y$  are the two orthogonal directions in the transverse plane.

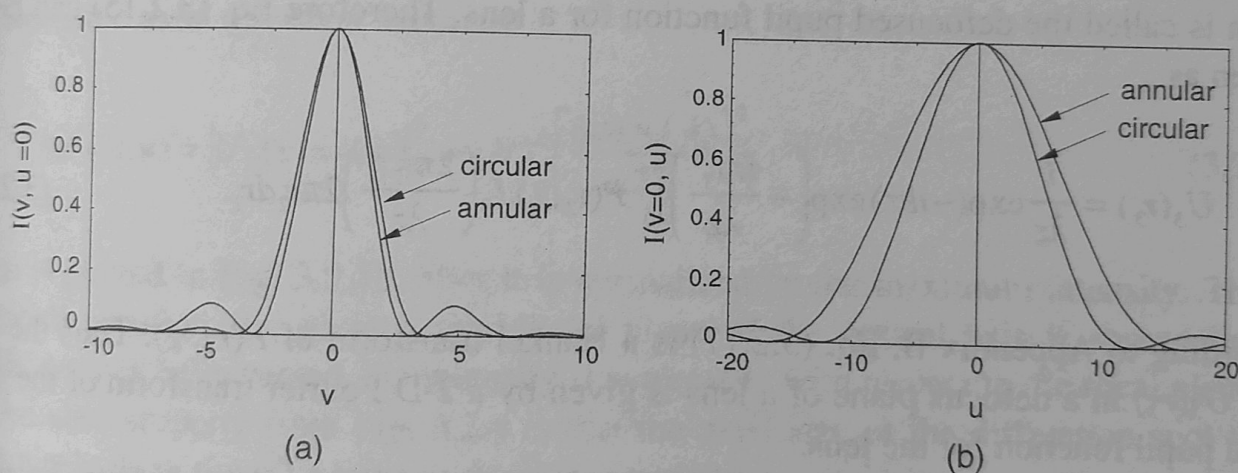


Fig. 3.2.5 Intensity distributions, normalized by the maximum intensity, along the radial direction in the focal plane (a) and along the optical axis (b) for a circular lens and an annular lens ( $\epsilon = 0.5$ ).

Eq. (3.2.14) is called the Airy pattern of a lens [3.2] and is shown in Fig. 3.2.4a. The intensity distribution, normalized by the maximum intensity, along the radial direction is depicted in Fig. 3.2.5a. Approximately 80% of the incident energy is confined to the central bright spot. The position at which the intensity drops to zero is approximately  $v = 3.83$ . Recalling Eq. (3.2.9), we can conclude that the central spot size is inversely proportional to the numerical aperture and directly proportional to the incident wavelength. These properties are important in determining image resolution; the smaller the central spot the higher image resolution.

To understand the diffraction pattern in a defocus plane by a circular lens, we substitute Eq. (3.2.6) into Eq. (3.2.4) and use polar coordinates, yielding

$$U_3(r_3) = \frac{i}{\lambda z} \exp(-ikz) \exp\left(-\frac{i\pi r_3^2}{\lambda z}\right) \int_0^\infty P(r_2) \exp\left[\frac{ikr_2^2}{2} \left(\frac{1}{f} - \frac{1}{z}\right)\right] J_0\left(\frac{2\pi r_2 r_3}{\lambda z}\right) 2\pi r_2 dr_2, \quad (3.2.15)$$

where the incident amplitude  $U_0$  has been assumed to be unity without losing generality. To simplify it, we let

$$P(r_2, z) = P(r_2) \exp\left[\frac{ikr_2^2}{2} \left(\frac{1}{f} - \frac{1}{z}\right)\right], \quad (3.2.16)$$

which is called the defocused pupil function for a lens. Therefore Eq. (3.2.15) can be rewritten as

$$U_3(r_3) = \frac{i}{\lambda z} \exp(-ikz) \exp\left(-\frac{i\pi r_3^2}{\lambda z}\right) \int_0^\infty P(r_2, z) J_0\left(\frac{2\pi r_2 r_3}{\lambda z}\right) 2\pi r_2 dr_2. \quad (3.2.17)$$

According to Appendix B, Eq. (3.2.17) is a Hankel transform of  $P(r_2, z)$ . Thus the light field  $U_3(r_3)$  in a defocus plane of a lens is given by a 2-D Fourier transform of the defocused pupil function for the lens.

In the present situation, the following two optical coordinates can be introduced.

a) Radial (transverse) optical coordinate  $v$ . Because a defocus plane is considered, the definition of  $v$  now becomes

$$v = \frac{2\pi a}{\lambda} \frac{a}{z} r_3 \approx \frac{2\pi a}{\lambda} \frac{a}{f} r_3 \approx \frac{2\pi}{\lambda} r_3 \sin \alpha, \quad (3.2.18)$$

b) Axial optical coordinate  $u$ :

$$u = \frac{2\pi}{\lambda} a^2 \left(\frac{1}{f} - \frac{1}{z}\right) \approx \frac{2\pi}{\lambda} \Delta z \frac{a^2}{f^2}. \quad (3.2.19)$$

Using  $v$  and  $u$  in Eq. (3.2.17) and expressing  $U_3$  as an explicit function of the defocus distance  $u$  gives

$$U_3(v, u) = 2iN \exp(-ikf) \exp\left(-\frac{iv^2}{4N}\right) \int_0^1 P(\rho) \exp\left(\frac{iu\rho^2}{2}\right) J_0(v\rho) \rho d\rho, \quad (3.2.20)$$

where  $\rho = r_2/a$ .

For a lens of a uniform circular aperture, Eq. (3.2.20) reduces to

$$U_3(v, u) = 2iN \exp(-ikf) \exp\left(-\frac{iv^2}{4N}\right) \int_0^1 \exp\left(\frac{iu\rho^2}{2}\right) J_0(v\rho) \rho d\rho. \quad (3.2.21)$$

This is an expression giving the 3-D distribution of the diffraction pattern near the region of the focal plane. In general,  $U_3(v, u)$  can be expressed by Lommel functions or evaluated by numerical integration [3.1]. When  $u = 0$ , i.e. when the observation plane is at the focus, the in-focus intensity is given by Eq. (3.2.14), as expected. When  $v = 0$ , the intensity along the axial direction becomes

$$I(v = 0, u) = |U_3(v = 0, u)|^2 = (N)^2 \left[ \frac{\sin(u/4)}{u/4} \right]^2, \quad (3.2.22)$$

which is plotted in Fig. 3.2.5b, after it is normalized by the maximum intensity. The intensity distribution  $I(v, u)$  in a meridional plane of the optical axis is shown in Fig. 3.2.4b. As may be expected, the intensity is symmetric with respect to the focal plane at  $z = f$ . Another property from Fig. 3.2.4 is that the axial size of the diffraction spot is approximately three times as large as the transverse size.

### 3.2.2 Annular Lens

An annular lens means that a circular opaque disk is co-axially placed in the aperture of a lens, so that the pupil function for an annular lens is given by

$$P(\rho) = \begin{cases} 1 & , \quad \varepsilon < \rho \leq 1, \\ 0 & , \quad \text{otherwise,} \end{cases} \quad (3.2.23)$$

where  $\varepsilon$  is the radius of the central obstruction normalized by the radius of the lens aperture,  $a$ . Using Eq. (3.2.23) in Eq. (3.2.20) yields